



IZTECH Open Access Articles

Developing a facile 1 method for highly luminescent colloidal CdSxSe1-x ternary nanoalloys†

The IZTECH Faculty has made this article openly available. **Please share** how this access benefits you. Your story matters.

Citation	Ünlü, C, Ünal, G, Sevim, S, and Özçelik, S, “ <i>Developing a facile 1 method for highly luminescent colloidal CdSxSe1-x ternary nanoalloys†</i> ” Journal of Materials Chemistry C © 2013 Royal Society of Chemistry
As Published	10.1039/c3tc00077j
Publisher	Royal Society of Chemistry
Version	PUBLISHED ARTICLE
Accessed	FRI JULY 5 16:52:32 GMT 2013
Citable Link	http://hdl.handle.net/11147/
Terms of Use	Article is made available in accordance with the publisher's policy and may be subject to Turkish copyright law. Please refer to the publisher's site for terms of use.
Detailed Terms	



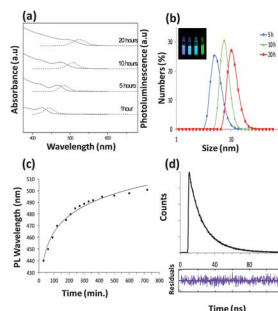
PAPER

1

Developing a facile method for highly luminescent colloidal CdS_xSe_{1-x} ternary nanoalloys

Caner Ünlü, Gülçin Ünal Tosun, Seçil Sevim and Serdar Özçelik*

3 We report a facile method to synthesize highly luminescent colloidal CdS_xSe_{1-x} ternary nanoalloys.



Please check this proof carefully. **Our staff will not read it in detail after you have returned it.**

Translation errors between word-processor files and typesetting systems can occur so the whole proof needs to be read. Please pay particular attention to: tabulated material; equations; numerical data; figures and graphics; and references. If you have not already indicated the corresponding author(s) please mark their name(s) with an asterisk. Please e-mail a list of corrections or the PDF with electronic notes attached – do not change the text within the PDF file or send a revised manuscript.

Please bear in mind that minor layout improvements, e.g. in line breaking, table widths and graphic placement, are routinely applied to the final version.

We will publish articles on the web as soon as possible after receiving your corrections; no late corrections will be made.

Please return your **final** corrections, where possible within **48 hours** of receipt by e-mail to: materialsC@rsc.org

Reprints—Electronic (PDF) reprints will be provided free of charge to the corresponding author. Enquiries about purchasing paper reprints should be addressed via: <http://www.rsc.org/publishing/journals/guidelines/paperreprints/>. Costs for reprints are below:

Reprint costs

No of pages

Cost (per 50 copies)

First

Each additional

2–4

£225

£125

5–8

£350

£240

9–20

£675

£550

21–40

£1250

£975

>40

£1850

£1550

Cost for including cover of journal issue:
£55 per 50 copies

Developing a facile method for highly luminescent colloidal $\text{CdS}_x\text{Se}_{1-x}$ ternary nanoalloys†

Caner Ünlü,‡ Gülçin Ünal Tosun,§ Seçil Sevim and Serdar Özçelik*

Cite this: DOI: 10.1039/c3tc00077j

We report a facile method to synthesize highly luminescent colloidal $\text{CdS}_x\text{Se}_{1-x}$ ternary nanoalloys. The synthesis is achieved exactly in one-step, one-pot and at low temperature, by applying the two-phase thermal approach. The optical and structural properties of the nanoalloys were characterized by various techniques. Photoluminescence of the nanoalloys is tunable from 435 to 545 nm by either the size or the composition of the nanoalloys. Highly luminescent nanoalloys having quantum yields up to 90% were prepared. The hydrodynamic size of the nanoalloys can be varied from 1.4 to 10.0 nm by the reaction time. DLS measurements showed that the size distribution of the nanoalloys is monodispersed. TEM images confirmed the size and the size distribution of the nanoalloys. The sulfur fraction in the nanoalloy composition, measured by XRD and verified by EDX, is modulated from 0.17 to 0.95 by increasing the amount of thiourea in the chalcogenide mixture. The sulfur-rich nanoalloys are formed when the initial mole ratio of the chalcogenide (S : Se) is equal or higher than eleven-fold. The gradient and homogeneous internal structures are revealed by analysis of the alloy composition as a function of the growth time. We propose that the two-phase approach, a non-injection technique, is a facile and versatile method to develop highly luminescent $\text{CdS}_x\text{Se}_{1-x}$ nanoalloys without an inorganic coating layer.

Received 12th January 2013

Accepted 18th March 2013

DOI: 10.1039/c3tc00077j

www.rsc.org/MaterialsC

Introduction

A pressing demand to produce highly luminescent colloidal semiconductor nanocrystals (quantum dots) urges scientists to invent novel synthetic chemistry.¹ Luminescent nanocrystals possessing higher quantum efficiency, narrower spectral emission and easy color tunability promise great potential as light emitting nanomaterials for next generation optoelectronic and biomedical applications.^{2–4} The requirements for the materials are significantly challenging for the next generation of displays, white light illuminators, solar cells, photo-detectors, image sensors, biosensors and drug delivery systems. Nanomaterials should be produced by low-cost and eco-friendly approaches.¹ In addition, the production rate of these materials should be kilograms per day to built next generation devices.

Research efforts have mainly focused on the development of binary semiconductor colloidal nanocrystals.^{5,6} The research concentrated on colloidal semiconductor alloyed nanocrystals (nanoalloys) has been recently reviewed.⁷ The adjustment of the

nanocrystal size is one way to tune the optical properties of the colloidal semiconductor nanocrystals. But, the size of the nanocrystals may lead to problems in some applications, especially in the life sciences. An alternative way of tailoring the optical properties is to adjust the composition of the nanocrystals. The cation-common alloys such as $\text{CdSe}_x\text{Te}_{1-x}$ (ref. 8) or the anion-common one like $\text{Zn}_x\text{Cd}_{1-x}\text{Se}$ (ref. 9) are examples of the ternary nanoalloys.

Accounts on the synthetic chemistry of colloidal $\text{CdS}_x\text{Se}_{1-x}$ nanoalloys are very limited. The first study on the synthesis of the colloidal $\text{CdS}_x\text{Se}_{1-x}$ nanoalloy was reported by Jang *et al.* in 2003.¹⁰ They prepared the nanoalloys at a very high temperature (300 °C) by swift injection of the mixture of S and Se tri-octylphosphine into cadmium oleate solution. The PL wavelength was tuned from 460 to 580 nm having quantum yields up to 85%. Moreover, they fabricated the nanoalloy based light emitting diodes, but the brightness and the external efficiency was very low.¹¹ Swafford *et al.* reported the synthesis of homogeneous alloys of $\text{CdS}_x\text{Se}_{1-x}$ by the hot-injection technique (315 °C).¹² The band gap of the nanoalloys was size and composition tunable. However, the PL of the nanoalloy showed defect-induced emission, causing low quantum yields. The synthesis of the nanoalloys at high temperatures (230–300 °C), with quantum yields in the range of 30–80% in various coordinating and non-coordinating solvents was achieved by Al-Salim *et al.*¹³ The reported PL range was from 490 to 620 nm. On the other hand, Ouyang *et al.* introduced a non-injection based approach for the synthesis of the $\text{CdS}_x\text{Se}_{1-x}$ nanoalloys, emitting in the

Department of Chemistry, Izmir Institute of Technology, Gülbahçe Köyü, Urla, 35430 Izmir, Turkey. E-mail: serdarozcelik@iyte.edu.tr; Fax: +90 232 750 75 09; Tel: +90 232 750 7502

† Electronic supplementary information (ESI) available. See DOI: 10.1039/c3tc00077j

‡ Current address: Biophysics Department, Wageningen U&R Dreijenlaan 3, Wageningen, The Netherlands, Fax: +31 317 482725; Tel: +31 317 482044.

§ Current address: Chemistry Department, University of Delaware, Delaware, USA.

1 range from 470 to 550 nm.¹⁴ But, the quantum yields of the
2 nanoalloys were quite low, below 5%. Chen *et al.* provided
3 another non-injection approach for the synthesis of the
4 CdS_xSe_{1-x} nanoalloy in aqueous solutions at 100 °C. The
5 quantum yield of the nanoalloys was again low, 3–14%
6 depending on the precursors used.¹⁵ The non-injection
7 methods reported for the synthesis appear to have difficulty
8 producing highly luminescent nanoalloys (quantum yield
9 having more than 50%). The hot injection approach has been
10 the most preferred method for the synthesis of the cation-
11 common nanoalloys. This approach, however, produces the
12 CdS_xSe_{1-x} nanoalloys with photoluminescence with quantum
13 yields varying in the range of 30–85%, and requires a high
14 temperature causing a lower production rate.

15 The materials' requirements for advanced technological
16 applications demand the development of highly luminescent,
17 colloidal nanocrystals produced at a lower temperature. Here,
18 we report the development of highly luminescent CdS_xSe_{1-x}
19 nanoalloys based on the two phase approach which is a non-
20 injection method for the synthesis. The reaction temperature
21 was kept at 100 °C to prepare the nanoalloys with higher
22 quantum yields and narrower emissions with pure colors. The
23 approach facilitates the synthesis in one step, one-pot, and at
24 low temperature and pressure. The optical properties of the
25 ternary CdS_xSe_{1-x} nanoalloys are tuned by either controlling the
26 composition or the size of the alloys. The developed method is
27 a facile procedure for the production of ternary or binary
28 quantum dot based nanomaterials.

30 Experimental

31 All of the chemicals used in this work were of the highest purity
32 and were purchased from the Sigma-Aldrich Co. They were used
33 without further purification.

34 Synthesis of cadmium myristate

35 The cadmium precursor was prepared by following the method
36 given by Pan *et al.*¹⁶ Typically, 10 mmoles of cadmium oxide
37 (CdO) and 20 mmoles of myristic acid were mixed and heated at
38 200 °C for ten minutes. The reaction was terminated when
39 a clear solution was obtained. Cadmium myristate (CdMA) was
40 recrystallized with toluene, dried at room temperature and
41 stored in the freezer.

42 Synthesis of NaHSe as the Se precursor

43 NaHSe was synthesized according to a previously published
44 procedure.¹⁷ Se powder (0.4 mmol) and NaBH₄ (1 mmol) were
45 mixed in a 5 ml reaction flask under N₂ atmosphere. Then 1 ml
46 of distilled water saturated by nitrogen was added to the reac-
47 tion media by a glass syringe. The resulting clear solution was
48 directly used without any further purification. In all experi-
49 ments, freshly synthesized NaHSe solutions were used.

50 Synthesis of the ternary CdS_xSe_{1-x} nanoalloys

51 The ternary CdS_xSe_{1-x} nanoalloys were synthesized by modi-
52 fying the two phase approach. 0.4 g cadmium myristate (CdMA)

53 and 2.0 g of oleic acid (OA) or tri-*n*-octylphosphine oxide (TOPO)
54 were dissolved in 80 ml toluene at 80 °C. NaHSe (3 mg) and
55 thiourea (60 mg) were co-dissolved in N₂ saturated water (80 ml)
56 and heated at 100 °C for 30 minutes under vigorous stirring.
57 CdMA and OA (TOPO) dissolved in toluene at 80 °C were added
58 to the hot aqueous solution of NaHSe and thiourea mixture. The
59 co-existence of Se and S precursors in this chalcogenide mixture
60 assured the formation of the nanoalloys. The colloidal
61 CdS_xSe_{1-x} nanoalloys begin to form within 15 minutes. Aliquots
62 were taken to monitor the progress of the nanoalloy formation
63 by using UV-Vis and fluorescence spectrophotometers, and DLS
64 measurements. The reaction was stopped by cooling the solu-
65 tion to room temperature when the pre-determined size was
66 reached. The nanoalloys were purified by precipitating the
67 crude solution with the addition of ethanol. The purification
68 procedure was repeated several times to remove unreacted
69 species and excess capping agents. This typical synthesis
70 procedure was used to control the size and the composition of
71 the nanoalloys by varying the reaction time and the initial
72 amount of thiourea, respectively. The reaction times and the
73 initial mole ratio of NaHSe and thiourea are provided in Tables
74 1 and 2, respectively.

75 Optical and structural characterization

76 The optical (spectral) and structural properties of the nano-
77 alloys were characterized by various techniques. All of the
78 measurements were conducted at room temperature. The
79 optical properties of the nanoalloys were measured at room
80 temperature by using Varian Cary 50 UV-Vis, and Varian Cary
81 Eclipse fluorescence spectrophotometers. A PTI-QM1 fluores-
82 cence spectrophotometer equipped with a Picoquant time-
83 correlated single photon counting unit was used for the lifetime
84 measurements. Quantum yields of the nanoalloys were
85 measured by using coumarin 6 in ethanol as a standard (the
86 reference quantum yield was 0.78). XRD measurements were
87 carried out with Panalytical X'Pert Pro Materials Research
88 Diffractometer with CuK α radiation ($\lambda = 1.5406 \text{ \AA}$). The XRD
89 data was collected in a step scanning mode in the range from
90 10° to 60°. The purified and powdered nanoalloys were used in
91 the XRD measurements and the elemental analysis (EDX).
92 Philips XL 30S FEG scanning electron microscope was used for
93 EDX analysis. DLS measurements were performed by Malvern
94 Zetasizer Nano ZS. High resolution transmission electron
95 microscope (HRTEM) images were obtained with a Zeiss 912
96 Omega microscope working at a voltage of 120 kV or a Technai
97 F20 microscope working at a voltage of 200 kV SFEG. TEM based
98 EDX analysis was also carried out.

99 Results

100 The size dependent optical properties

101 The optical properties of the colloidal nanoalloys could be
102 modulated by the size and composition of the alloys. The
103 optical properties of the nanoalloys were monitored by
104 sampling during the reaction progression. Fig. 1 represents the
105 optical and structural properties, as well as the temporal

Table 1 The optical properties of the CdS_{0.75}Se_{0.25} nanoalloy capped by oleic acid^a

Time (h)	Size (nm)	E_g (eV)	λ_{Abs} (nm)	λ_{PL} (nm)	Stokes shift (nm)	FWHM (nm)	QY (%)
1	1.4 ± 0.4	2.7	423	445	22	29	45
5	4.9 ± 1.4	2.5	466	485	19	30	75
10	7.2 ± 1.6	2.4	476	505	29	36	90
20	10.1 ± 2.1	2.3	495	525	30	40	80

^a The initial chalcogenide mole ratio was 1 : 22. The composition of the nanoalloy CdS_{0.75}Se_{0.25} was determined by XRD and verified by EDX. The hydrodynamic size was measured by DLS.

evolution of the nanoalloy CdS_{0.75}Se_{0.25} (determined by XRD and verified by EDX) capped by oleic acid (OA). Fig. 1a shows the typical absorption and photoluminescence (PL) spectra of the CdS_{0.75}Se_{0.25} nanoalloys sampled at different reaction times varying from 1 hour to 20 hours. The absorption maxima were varied from 423 nm to 495 nm while the peak positions of the PL spectra were shifted from 445 nm to 525 nm when the reaction time was longer (the larger the size). Shoulders or broader bands in the PL spectra were not observed at all. The Stokes shift increased gradually with a longer reaction time. The full width at half maxima of the PL spectra was about 30–40 nm. The sizes of the nanoalloys were measured by DLS as represented in Fig. 1b. The hydrodynamic size of the nanoalloy was small; 1.4 nm at one-hour and then reaching up to 10.0 nm at the end of twenty hours of reaction time (Table 1). It was noted that the size distributions were quite narrow, indicating monodispersity. The photograph inset in Fig. 1b shows the true emission colors of the nanoalloys under UV-radiation. The quantum yields were increased from 45% to 90% by increasing the size, however a little decrease in the yield was observed as the nanoalloy was grown to 10.0 nm (Table 1). The energy band gap (E_g) calculated from the UV-Vis. spectra was reduced from 2.7 eV to 2.3 eV as the size increased, verifying the quantum confinement effect. The temporal evolution was monitored by the shift of the PL maxima as shown in Fig. 1c. The PL spectra of the oleic acid capped nanoalloy were shifted to higher wavelengths in time, evidence of the increase of the hydrodynamic size. The shift became steady at approximately 5 hours for the nanoalloys capped with OA. Fig. 1d shows a characteristic PL decay curve of the nanoalloy. The decay times were best described by a three-exponential fit with lifetime components of $\tau_1 \sim 17\text{--}22$ ns, $\tau_2 \sim 6$ ns and $\tau_3 \sim 0.6$ ns along with acceptable statistics ($\chi^2 < 2.0$). The amplitudes of the components were

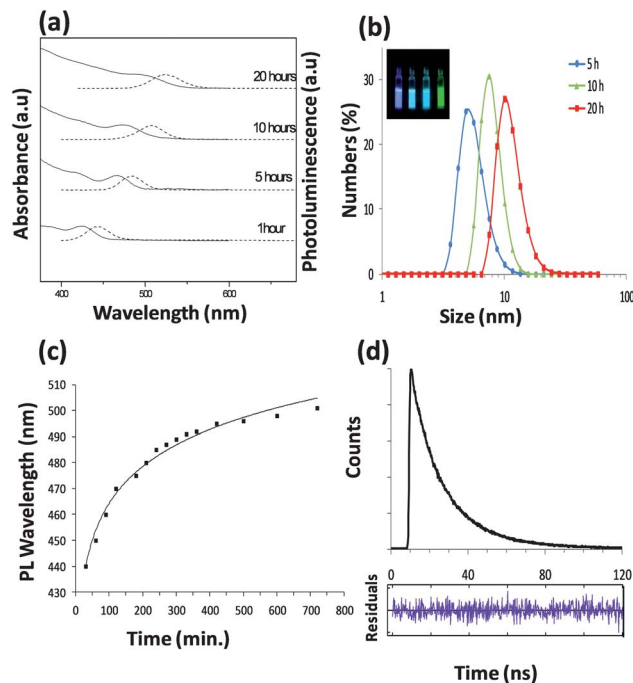


Fig. 1 (A) Absorption and PL spectra of CdS_{0.75}Se_{0.25} nanoalloys capped by oleic acid, grown at various reaction times: 1–20 hours. (B) Size distribution of the nanoalloys grown at various hours. The inset is the emission color photograph of the nanoalloys under UV illumination (366 nm). (C) Temporal evolution of the nanoalloys. (D) A representative luminescence decay curve of the nanoalloy.

approximately equal to each other. The component of the longest decay time was systematically shortened from 22.5 ns to 17.4 ns, as the size increased. As a result, the average decay time decreased from 9.5 ns to 7.9 ns. All of the findings that were

Table 2 The structural and optical properties of the CdS_xSe_{1-x} nanoalloys. TOPO was used as the surfactant. The growth time was fixed at 5 hours

Mole ratio of Se : S	Composition		Size (nm)			Optical properties		
	XRD	EDX	XRD	TEM	DLS	λ_{Abs} (nm)	λ_{PL} (nm)	QY (%)
1 : 7	CdS _{0.17} Se _{0.83}	CdS _{0.24} Se _{0.76}	1.9	1.9	5.5 ± 2.0	458	475	56
1 : 11	CdS _{0.50} Se _{0.50}	CdS _{0.50} Se _{0.50}	1.9	—	5.9 ± 2.1	466	484	52
1 : 22	CdS _{0.75} Se _{0.25}	CdS _{0.75} Se _{0.25}	2.0	2.0	5.9 ± 2.1	487	512	61
1 : 33	CdS _{0.92} Se _{0.08}	—	2.5	—	6.2 ± 2.4	515	535	56
1 : 55	CdS _{0.95} Se _{0.05}	CdS _{0.94} Se _{0.06}	2.5	2.5	6.2 ± 2.4	523	545	52

summarized in Table 1 indicated that the optical properties of the nanoalloy $\text{CdS}_{0.75}\text{Se}_{0.25}$ were tuned by the size.

The compositional tunable optical properties

It is expected that the optical properties of the nanoalloys could be tuned by the composition. The initial chalcogenide mole ratio of Se : S was systematically varied by increasing the amount of sulfur in the mixture. The adjustment of the mole ratio was realized by increasing the amount of thiourea while keeping the amount of NaHSe constant in the chalcogenide mixture (Table 2). Fig. 2a shows progressive shifts in the diffraction angles when the amount of thiourea in the initial mixture was increased, resulting in a change in the composition of the nanoalloy. When the amount of thiourea was higher the XRD patterns shifted to the bulk CdS diffraction angles, depicted as the dashed lines in Fig. 2a. The dashed lines represent the planes for the bulk single crystals of the CdS (JCPDS no. 10-0454) and the CdSe (JCPDS no. 19-0191). The peak position associated with the (111) plane has been progressively shifted to higher diffraction angles, as depicted in Fig. 2a.

The diffraction angles related to the other planes, the (220) and (311), were shifted as well, but this was less pronounced due to the ultra small size of the nanocrystals. The shift of the XRD patterns indicated that the fraction of sulfur incorporated

in the nanoalloys was increased. Since the lattice mismatch between CdS and CdSe is very small (3.9%),¹³ the composition of the $\text{CdS}_x\text{Se}_{1-x}$ nanoalloys can be calculated by Vegard's law. The compositions of the nanoalloys were inserted in Fig. 2a, as well as given in Table 2. The plot of the nanoalloy compositions *versus* the initial chalcogenide mole ratios was found to be nonlinear as illustrated in Fig. 2b. There is a sharp increase in the plot when the initial chalcogenide ratio is 1 : 33. When the initial chalcogenide ratio was 1 : 7, the selenium-rich nanoalloy $\text{CdS}_{0.17}\text{Se}_{0.83}$ was formed. When the initial chalcogenide ratio was 1 : 11, the sulfur and selenium fractions in the nanoalloy were equal to each other. This finding suggests that the selenium ions are eleven times more reactive than the sulfur ions towards cadmium ions. When the amount of sulfur was equal or higher than 22-fold, the nanoalloy became a sulfur-rich nanoalloy, the fraction varied from 0.75 to 0.95. Fig. 2c illustrates the optical spectra of the nanoalloys with various compositions. The spectra were shifted to higher wavelengths when the sulfur fraction incorporated in the nanoalloy was higher. The DLS data inserted in Fig. 2c verified that the size of the nanoalloys remained almost constant. Table 2 summarizes the optical and structural parameters of the nanoalloys having a hydrodynamic size around 5.0 nm. The crystalline size of the nanoalloys determined by HRTEM was around 2.0 nm. The DLS and TEM data differ because DLS contains scattering from surfactants and solvent molecules surrounding the crystalline size of the nanoalloys.

The variation in the composition of the nanoalloys is anticipated to regulate the photoluminescent properties. Fig. 3 illustrates how the composition tunes the PL spectra of the $\text{CdS}_x\text{Se}_{1-x}$ nanoalloys. The shape of the PL spectra of the nanoalloys was the same; a single emission band. The PL maxima were tuned from 475 to 545 nm by adjusting the fraction of sulfur incorporated in the nanoalloys ranging from 0.17 to 0.95. For comparison purposes, the binary CdS and CdSe nanocrystals were also prepared by the two phase-method. It was observed that CdS and CdSe nanocrystals at the same size as the nanoalloys exhibited emissions, centered at 425 and 435 nm respectively, along with additional broad emission features presumably arising from the surface-trap states. However, this broad feature completely disappeared in the PL spectra of the nanoalloys.

It was noted that the PL wavelength maxima of the nanoalloys were not in the spectral range of the binary CdS and CdSe nanocrystals. This will be discussed in the next section. The relationship between the PL maxima and the chalcogenide ratio S represented in Fig. 3b, is nonlinear. The shift in PL wavelength is small for the selenium rich nanoalloy. Substantial red-shifts are evident for the sulfur rich nanoalloys. This nonlinear effect is in harmony with the results determined by XRD measurements, which indicated the nonlinear relation between the nanoalloy composition and the initial mole ratio of the chalcogenides. The PL quantum yields of the nanoalloys capped with TOPO were measured to vary from 52 to 61%, suggesting the high quality of the nanoalloys. It should be noted that there was no inorganic coating layer, like ZnS or CdS, to protect the nanoalloys. It is remarkable that the quantum yields

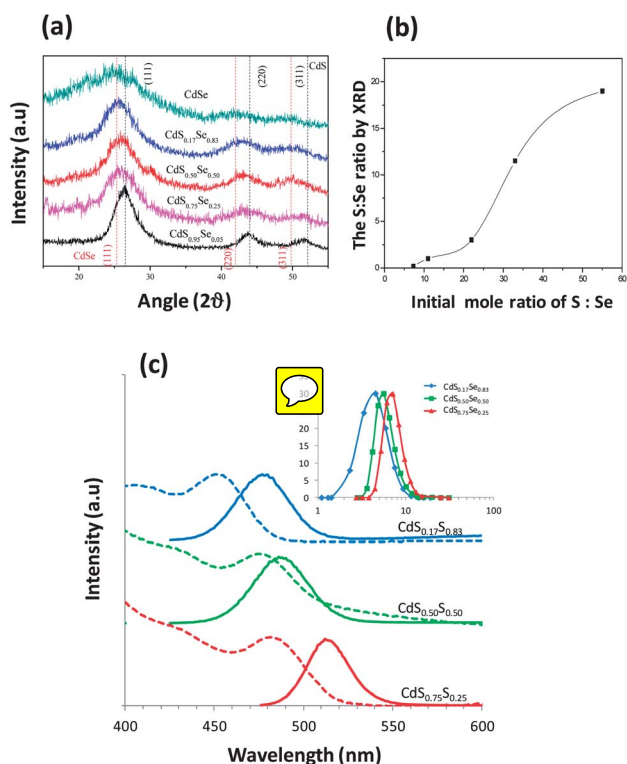


Fig. 2 (A) XRD diffractogram of the $\text{CdS}_x\text{Se}_{1-x}$ nanoalloys synthesized with different initial Se : S ratios. Vegard's law was used for the determination of the fractions of Se and S given in the formula. (B) A plot of the initial S ratio *versus* the S ratio in the nanoalloy determined by XRD. (C) Optical spectra and the size distribution of the nanoalloys with different initial Se : S ratios.

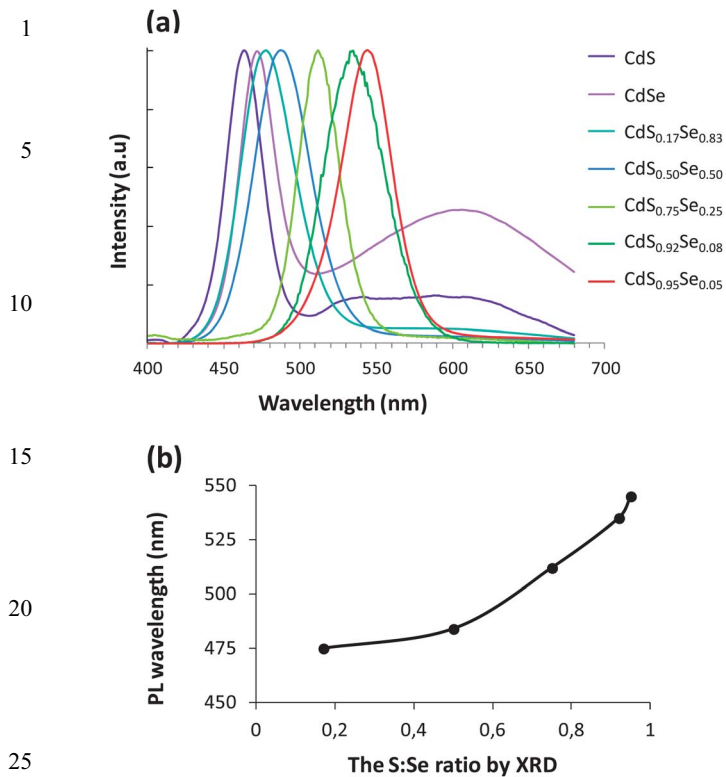


Fig. 3 (A) PL spectra of the CdS_xSe_{1-x} with different fractions of Se : S incorporated. The CdS and CdSe at the same size as the nanoalloys are provided for comparison. (B) A plot of the PL wavelength vs. the S : S + Se ratio in the nanoalloy.

were not significantly changed by the composition as opposed to the size. The nanoalloys with lower chalcogenide ratios, such as 1 : 1 to 1 : 3, were prepared, but their quantum yields were very low, typically less than 5%.

Typical TEM images and energy dispersive X-ray spectrum (EDX) of the nanoalloys are presented in Fig. 4. It was observed that the CdS_xSe_{1-x} nanoalloys are spherical and the size distribution is monodispersed, confirming the DLS measurements. The crystalline sizes of the CdS_xSe_{1-x} nanoalloys grown at 5 and 20 hours were respectively measured to be 2.0 and 5.0 nm, as illustrated in Fig. 4a. The crystalline and hydrodynamic sizes of the nanoalloys measured by the two different techniques agreed with each other very well. HRTEM images depict the crystalline planes of the nanoalloys having a zinc blend cubic structure. The intensity distribution of the HRTEM images suggests the homogeneous internal structure of the nanoalloys. Fig. 4b represents an EDX spectrum confirming the presence of Cd, Se and S in the nanoalloys. C, O and P peaks in the EDX spectra originate from the surfactant molecules, TOPO. It must be noted that EDX analysis provides qualitative information for the nanoalloy composition. The EDX results, even though qualitative, agreed very well with the results determined by the XRD analysis.

The variation in the nanoalloy composition as a function of the growth time was monitored to better understand the internal structure of the nanoalloys. The unreacted precursors

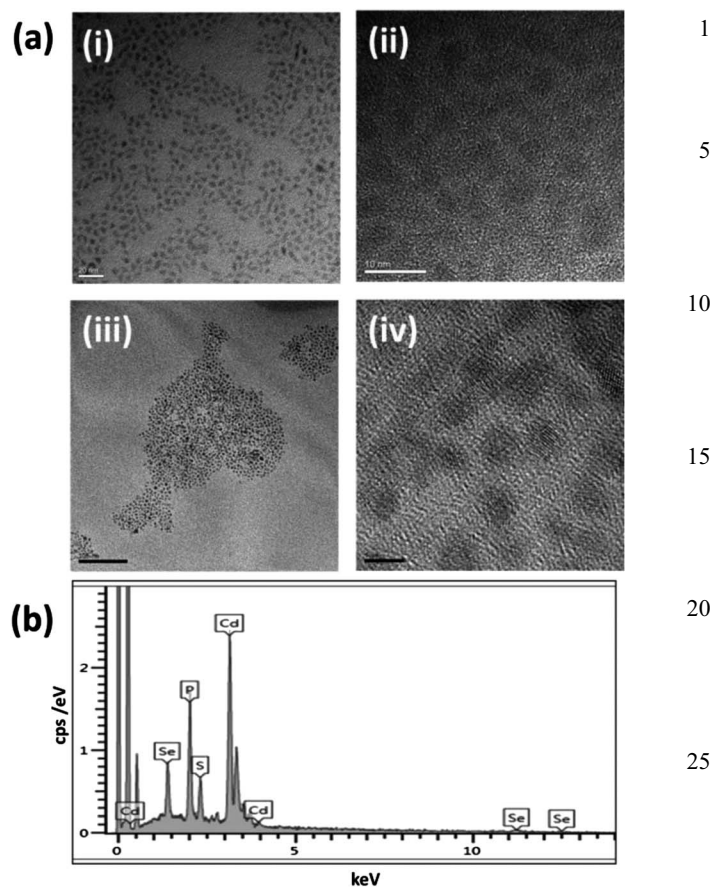


Fig. 4 (A) TEM images of the CdS_xSe_{1-x} nanoalloys, (i) 5.0 nm sized CdS_xSe_{1-x} nanoalloys, (ii) HRTEM of the 5.0 nm sized CdS_xSe_{1-x} nanoalloys, (iii) 2.0 nm sized CdS_xSe_{1-x} nanoalloys and (iv) HRTEM of the 2.0 nm sized CdS_xSe_{1-x} nanoalloys. (B) EDX spectra of a CdS_xSe_{1-x} nanoalloy coated with TOPO.

were removed from the samples by successive purification steps before the EDX analysis. Fig. 5 demonstrates the variation of the compositions of the nanoalloys CdS_{0.24}Se_{0.76} and CdS_{0.75}Se_{0.25} as a function of the growth time. The composition was almost equally incorporated into the alloy after 3 hours of growth when the initial mole ratio of Se : S was 1 : 7, corresponding to the nanoalloy CdS_{0.24}Se_{0.76}. After 3 hours of growth, the selenium percent increased steadily in the nanoalloy composition, resulting in a selenium richer gradient alloy at 10 hours. On the other hand, when the initial mole ratio of Se : S was 1 : 22, the composition remained the same during the growth, implying the uniform growth of the nanoalloy. These findings suggest that the internal structure may be affected by the initial mole ratio and the reactivity of the chalcogenide precursors toward cadmium ions, which is in excess.

Discussion

The synthesis of the nanoalloys

The two phase thermal approach was introduced by Brust *et al.* to synthesize metallic nanocrystals at the interface of two liquid phases.¹⁸ Pan *et al.* explored the two-phase approach to synthesize colloidal binary CdSe–CdS core–shell nanocrystals

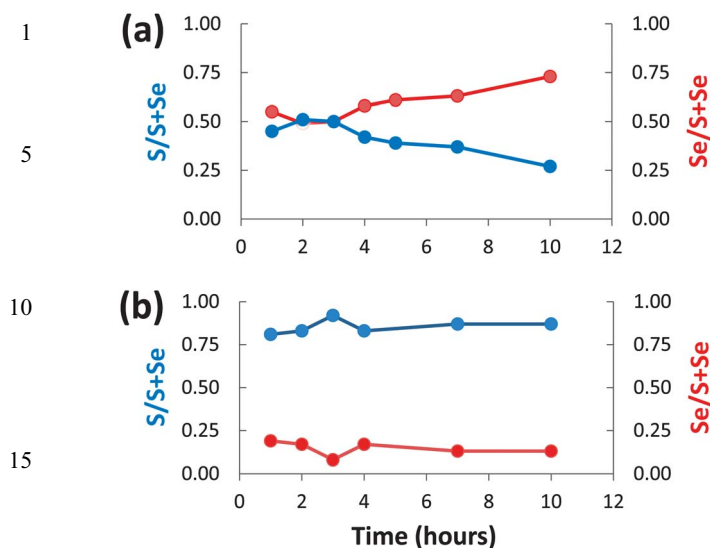


Fig. 5 Variation in the nanoalloy composition, determined by EDX, as a function of the growth time. (A) The nanoalloy CdS_{0.24}Se_{0.76} forms a selenium-rich gradient alloy. (B) The composition of the nanoalloy CdS_{0.75}Se_{0.25} remains uniform with the growth time, forming a homogeneous alloy.

having quantum yields up to 80%.^{16,19–21} The formation of the ternary nanoalloys like CuInS₂ and CuInSe₂ by the two-phase method was proposed but not demonstrated.²² The approach has not been applied to synthesize the ternary CdS_xSe_{1–x} nanoalloys as well.

To emphasize the modification of the synthesis in this study, it is crucial to briefly describe the synthesis achieved by Pan *et al.* for the CdSe–CdS core–shell nanocrystals. It was a two-step method. *In the first step*, the CdSe core was prepared in an autoclave by mixing CdMA in OA–toluene and selenourea in water. The mixture was heated and maintained at 180 °C for a period of time to develop CdSe nanocrystals in a desired size. *In the second step*, the crude solution of CdSe was firstly purified by precipitation and decantation. Then, the purified nanocrystals were redissolved in OA–toluene and a calculated amount of CdMA, depending on the shell thickness to be grown, was added to the solution. At last, the fresh aqueous solution of thiourea was mixed with the CdSe solution. The final mixture was transferred to the autoclave and maintained at 140 °C for the growth of the CdS shell layer. As summarized here, this synthesis procedure requires multiple steps and is totally different to what we developed for the synthesis. As we simply add, CdMA–OA (or TOPO) solution to the aqueous mixture of NaHSe and thiourea, the nanoalloys at the water–toluene interface are explicitly formed in one-step, one pot and at low temperature.

The procedure developed in this study reduces the number of steps necessary to synthesize the nanoalloys. This modification creates an economically and industrially-friendly production approach. This is important for the production of high quality nanomaterials to be used in advanced optoelectronic and biomedical devices. In addition, since the main constituent of the olive oil is oleic acid (55–83%), the method may be


considered eco-friendly; of course, cadmium has to be replaced to assume complete safety of the nanoalloys.

In this study, we used cadmium myristate in excess, thiourea and NaHSe as the chalcogenides because of their slow and fast reactivities towards cadmium ions. NaHSe was reported to have the fastest decomposition rate producing selenium ions among the precursors, such as selenourea, Na₂SeSO₃ and NaHSe.¹⁹ It was reported that selenourea and Na₂SeSO₃ are the choice for the slow nucleation and the slow growth of the binary nanocrystals. If a fast nucleation and fast growth is desired NaHSe is the preferred precursor. It was reported that the reactions with the slower selenium precursors were reproducible and controllable.¹⁹ However, we demonstrated that the growth of the nanoalloys by using NaHSe can be extended over 24 hours, which is attributed to the existence of an excessive amount of thiourea (up to 55 moles higher sulfur than selenium) in the reaction medium. The higher amount of thiourea hinders the faster diffusion of the selenium ions and, in turn, limits their availability around the cadmium ions. By adjusting the initial chalcogenide ratio (Se : S), it is practical to grow very small sized and highly luminescent nanoalloys emitting blue/green colors, from 425 to 540 nm. This very wide spectral range cannot be easily covered by the binary CdS or CdSe nanocrystals. For example, to prepare the nanocrystals emitting at 480 nm (the band gap of 2.6 eV), the CdS nanocrystals have to be very large, about 10 nm, while the CdSe nanocrystals should be extremely small, around 2.0 nm. These requirements may not be easily fulfilled; demonstrating the difficulty to adjust the PL wavelengths specifically in the blue/green region for cadmium based binary nanocrystals.

The amounts of reactants and their reactivity are two competing parameters that may play an important role in the fate of the synthesis and the quality of products. The formation of a selenium rich nanoalloy CdS_{0.17}Se_{0.83} validates the method for the nanoalloy formation, even in the presence of excess sulfur ions. The fraction of sulfur and selenium incorporated in the nanoalloy is equal when the initial chalcogenide ratio of Se : S is adjusted to 1 : 11, the critical ratio. When the amount of thiourea is more than the 11-fold, the sulfur rich nanoalloys are formed. The selenium rich nanoalloy is only formed when the chalcogenide ratio is less than the critical ratio.

The distribution of chalcogenide atoms (the internal structure) in the nanoalloys could be uniform or gradient type.⁷ HRTEM results suggest that the internal structure of the ternary CdS_xSe_{1–x} nanoalloy is homogeneous. It should be noted that it is not simple to observe the distribution and location of selenium and sulfur atoms in the nanoalloy due to their very close lattice constants. The optical features such as narrower emission bandwidth, higher quantum yields and no trap emission favor the homogeneous internal structure of the CdS_xSe_{1–x} nanoalloys. Swafford *et al.* reported that the composition of the CdS_xSe_{1–x} nanoalloys remained reasonably constant over the growth period for all the Se : S ratios, establishing the homogeneous nanoalloy.¹² Ouyang *et al.* also suggested the formation of the homogenous nanoalloys.¹⁴ In addition, we noted that the excess amount of cadmium ions assured that the surface of the nanoalloys should be terminated with cadmium ions

1 facilitating bonding with the ligands, thus protecting the
emitting part of the nanoalloys, resulting in highly luminescent
quantum dots.


5 To preserve the uniform size distribution and to prevent
agglomeration of the $\text{CdS}_x\text{Se}_{1-x}$ nanoalloys, surfactants are
generally exploited during the synthesis. In the hot injection
method, TOP and TOPO are generally preferred as the surfac-
tants,^{10,23–25} meanwhile oleic acid is the preferred surfactant in
10 the two phase method.^{16,19–21,26–29} We showed that both TOPO
and oleic acid can be used in the synthesis of the nanoalloys.
Furthermore, the growth rate of the nanoalloys can be
controlled with the surfactants. The growth of the nanoalloys
coated with TOPO saturates at about 5 hours; however, the
15 growth with oleic acids slows down at about 15 hours. Similarly,
the influence of various solvents on the growth rate of the
nanoalloys was reported by Al-Salim *et al.*¹³ Both surfactants
have their own advantages. Oleic acid resulted in higher
quantum yields (up to 90%) compared to TOPO (up to 60%).
20 However, when TOPO is used, it makes it easier to exchange
TOPO with appropriate surface capping agents such as mercap-
to-propionic acid (MPA), or ethyl-*N*-cysteine (NAC) to
redisperse the nanoalloys in water, a requirement for biological
and biomedical studies.

25 The optical properties of the nanoalloys

The photoluminescence quantum yield is one of the important
optical parameters. The non-injection methods produced
30 nanoalloys that have low quantum yields, up to 14%. Since the
method we applied is basically a non-injection method, the
approach we used facilitates higher quantum yields from 45 to
90%, producing highly luminescent nanomaterials. The repor-
ted quantum yields of the $\text{CdS}_x\text{Se}_{1-x}$ nanoalloys vary from 3 to
35 85% depending on the synthesis methods.^{10,12–15} It was reported
that the structural disorder induced by the excessive sulfur
incorporated into the alloy reduced the quantum yield.³⁰ But,
the disorder was not imaged even when the Z-STEM technique
was exploited. Moreover, it was reported that the faster non-
40 radiative recombination processes resulted in the shorter the
lifetimes, below 30 picoseconds.³⁰ The average lifetimes of the
nanoalloys we developed were about 10 ns. This substantial
difference along with the higher quantum yields we obtained
indicates that the structure of the $\text{CdS}_x\text{Se}_{1-x}$ nanoalloys is less
45 defective due to slower growth at low temperature.

The binary nanocrystals synthesized by the two-phase
method using NaHSe have quantum yields up to 10% for CdSe,
50 and 30–40% for the CdSe–CdS nanocrystals.¹⁹ When selenourea
and thiourea were used the quantum yield increased up to 80%
depending on the core size and the shell thickness.¹⁶ The
optimized core size and the shell thickness were respectively 1.5
nm and a 0.6 monolayer. The core size played a decisive role in
improving the quantum yield of the CdSe–CdS binary nano-
55 crystals, but the thicker CdS shell reduced the QY. We report
the quantum yields up to 90% for the size-controlled nanoalloys.
The quantum yield was enhanced by a factor of two compared to
the binary core–shell nanocrystals using the same precursors
and the synthesis approach. The quantum yield for the

1 composition tuned nanoalloys is about 60% and almost
constant with the sulfur incorporated into the nanoalloy. This
finding may positively contribute to the hypothesis of the
homogeneous distribution of the chalcogenide atoms across
5 the nanoalloy. We note that the magnitude of the quantum yield
is lowered (down to 80%, Table 1) when the size is increased to
10 nm, the larger surface area may introduce surface defects
reducing the radiative rate constant which correlates with the
shorter lifetime values measured.

The photoluminescence wavelength is a very important
10 optical parameter. It can be controlled in two ways; tuning the
size or adjusting the composition of the nanoalloys. The spectra
of the $\text{CdS}_x\text{Se}_{1-x}$ nanoalloys were shifted to higher wavelengths
with increasing size with a constant composition. This was
15 anticipated due to the quantum confinement effect. The
adjustment of the PL wavelength by the composition of the
nanoalloy was also presented in this study. The PL spectra were
shifted to red as the sulfur fraction increased in the nanoalloy,
an unexpected result. It was presumed that the PL maxima of
20 the nanoalloys should be within the spectral region defined by
the parent binary CdS and CdSe nanocrystals at the same size.
However, the type of relationship between the composition and
the spectral properties is not what we expected. This fact is
attributed to the internal structure that promotes the exciton
25 leakage towards the exterior of the nanoalloy. As a result, it
extends the exciton delocalization and thus causes the red-shift
in the spectra. The exciton leakage has been reported for the
CdSe–CdS and CdSe–ZnS nanocrystals.^{24,31} Very recently,
CdSe–ZnS alloyed nanocrystals with an equal fraction of sulfur
30 and selenium incorporated in the alloy have been reported.³²
There was a small red shift when the ZnS shell was grown on the
core CdSeS. The optical bowing as the origin of the nonlinear
behavior of the spectral shift (mainly the band-gap tunability),
was observed for the alloys $\text{CdSe}_x\text{Te}_{1-x}$ and $\text{CdS}_x\text{Te}_{1-x}$ (ref. 8
35 and 33) The optical bowing in these alloys was attributed to the
large difference in the lattice constants of these alloys. Because
the difference in the lattice constants of CdS and CdSe is
insignificant (3.9%) and furthermore, the crystalline size is very
small (<2.5 nm) for the $\text{CdS}_x\text{Se}_{1-x}$ nanoalloys, the exciton
40 leakage may therefore be considered to be the origin of the
optical nonlinearity in our case  selenium-rich core and
sulfur-rich shell type structure remains as a possibility, but the
analysis of the internal structure denies that possibility.

45 The internal structure

The internal structure of the nanoalloys was estimated by the
analysis of the EDX spectra as a function of the growth time. We
50 found out two types of alloys: a gradient alloy and a homoge-
neous alloy (Fig. 6). Since we demonstrated the reactivity of the
precursors is pivotal to determine the composition of the
nanoalloy, this fact may be valid for the internal structure as
well. Since the reactivity of selenium ions is eleven times higher
55 than sulfur ions toward cadmium, we may expect the formation
of a selenium-rich gradient alloy. When the chalcogenide molar
ratio is above eleven, then the reactivity and the mole ratio of
the chalcogenides begin to compete for the fate of the alloy type.

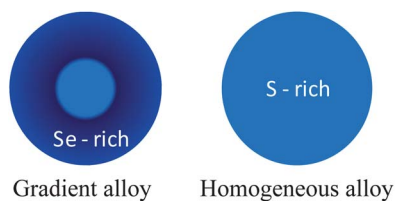


Fig. 6 A schematic representation of the two types of nanoalloys. The gradient nanoalloy is selenium-rich but the homogenous alloy is sulfur rich.

The findings allow us to consider that the homogeneous internal structure of the nanoalloy is formed when the reactivity and the mole ratio of the chalcogenides are balancing each other. This proposal is supported by the observed composition dependent spectral shifts in the PL maxima of the nanoalloys. The shift in PL maxima is small for the gradient alloy, and for the homogeneous alloy the shift is larger. These observations are in agreement with the findings reported by Bailey and Nie for the alloy $\text{CdSe}_x\text{Te}_{1-x}$ which has both gradient and homogeneous internal structures.⁸ Swafford *et al.* reported the internal structure of the homogenous alloyed $\text{CdS}_x\text{Se}_{1-x}$ and the band-gap dependence to the composition. However, any connection between the composition and the PL properties was not discussed. The composition and location of sulfur ions in CdSse alloyed nanocrystals grown by the thermal decomposition from $[\text{Cd}_{10}\text{Se}_4(\text{SPh})_{16}]$ were reported by Lovingood *et al.*³⁶ They proposed a gradient alloy model in which a selenium-rich core is surrounded by a sulfur-rich layer. The proposed model by them is different to what we suggested. The contrast between both proposals is mainly based on differences of the precursors used in these studies and on the parameters that control the compositions. It is clear that the mechanisms related to the formation of alloys at the nanometer scale ought to be studied. Mechanistic studies are of importance because we urgently need to develop reactors for the large scale production of nanocrystals.

Demonstration of applications

Finally, so as to demonstrate applications of the nanoalloys, we exchanged the capping agent TOPO with mercaptopropionic acid (MPA), and we tracked the motions of the nanoalloy $\text{CdS}_{0.75}\text{Se}_{0.25}$ in a live-cell (the cell lines of A549 and BEAS2B) environment, and in real time. Some of the findings are presented in the ESI† part of this paper. The detailed results will be published elsewhere. In addition, the nanoalloy $\text{CdS}_{0.75}\text{Se}_{0.25}$ coated with TOPO was blended with MEH-PPV to fabricate a hybrid PLED device.³⁴ In the cited work, the nanoalloys enhanced electron injection and played a role as a hole blocker in separate devices. We furthermore showed control of spontaneous emission originating from nanocrystals embedded in electrospun nanofibers.³⁵

Conclusion

We showed that the two phase approach can be applied to synthesize colloidal, ternary $\text{CdS}_x\text{Se}_{1-x}$ nanoalloys in one-step,

one-pot and at low temperature. The hydrodynamic size of the nanoalloys is tunable by the reaction time, up to 10.1 nm. The fraction of sulfur incorporated in the nanoalloy can be adjusted from 0.17 to 0.95 by increasing the initial amount of thiourea, and by optimizing the reactivities of sulfur and selenium ions toward cadmium ions, as a result of precursor choices. The internal structure of the nanoalloys varies with the initial mole ratio and the reactivity of chalcogenides towards cadmium ions. We demonstrated that the optical properties of the $\text{CdS}_x\text{Se}_{1-x}$ nanoalloys can be tuned by either the composition or the size of the nanoalloys. The nanoalloys are highly luminescent in the blue/green region. Since the nanoalloy formation takes place at the interface between the two phases, this approach is superior over the hot injection method in terms of reproducibility, monodispersity and colloidal stability. This approach therefore may facilitate large scale manufacturing of the ternary colloidal semiconductor nanoalloys, leading to kg per day production. We propose that the modified two-phase approach is a facile method to produce highly luminescent nanoalloys for optoelectronic and biomedical applications.

Acknowledgements

This work was partially supported by a grant (code no. 108T446) from the Scientific and Technological Research Council of Turkey (TUBITAK), and the State Planning Organization of Turkey. We thank the specialists of the Iztech-Center for Materials Research, and Ingo Lieberwirth of MPI-I for HRTEM.

Notes and references

- 1 NANO futures, Integrated Research and Industrial Roadmap for European Nanotechnology, 2012, DLAS 2481.
- 2 T. Nann and W. M. Skinner, *ACS Nano*, 2011, **5**, 5291–5295.
- 3 N. Hildebrandt, *ACS Nano*, 2011, **5**, 5286–5290.
- 4 X. Michalet, F. F. Pinaud, L. A. Bentolila, J. M. Tsay, S. Doose, J. J. Li, G. Sundaresan, A. M. Wu, S. S. Gambhir and S. Weiss, *Science*, 2005, **307**, 538–544.
- 5 D. V. Talapin, J. S. Lee, M. V. Kovalenko and E. V. Shevchenko, *Chem. Rev.*, 2010, **110**, 389–458.
- 6 S. E. Lohse and C. J. Murphy, *J. Am. Chem. Soc.*, 2012, **134**, 15607–15620.
- 7 M. D. Regulacio and M. Y. Han, *Acc. Chem. Res.*, 2010, **43**, 621–630.
- 8 R. E. Bailey and S. M. Nie, *J. Am. Chem. Soc.*, 2003, **125**, 7100–7106.
- 9 X. H. Zhong, M. Y. Han, Z. L. Dong, T. J. White and W. Knoll, *J. Am. Chem. Soc.*, 2003, **125**, 8589–8594.
- 10 E. Jang, S. Jun and L. Pu, *Chem. Commun.*, 2003, 2964–2965.
- 11 S. Jun, E. J. Jang, J. Park and J. Kim, *Langmuir*, 2006, **22**, 2407–2410.
- 12 L. A. Swafford, L. A. Weigand, M. J. Bowers, J. R. McBride, J. L. Rapaport, T. L. Watt, S. K. Dixit, L. C. Feldman and S. J. Rosenthal, *J. Am. Chem. Soc.*, 2006, **128**, 12299–12306.
- 13 N. Al-Salim, A. G. Young, R. D. Tilley, A. J. McQuillan and J. Xia, *Chem. Mater.*, 2007, **19**, 5185–5193.

- 14 J. Y. Ouyang, M. Vincent, D. Kingston, P. Descours, T. Boivineau, M. B. Zaman, X. H. Wu and K. Yu, *J. Phys. Chem. C*, 2009, **113**, 5193–5200.
- 15 X. F. Chen, J. L. Hutchison, P. J. Dobson and G. Wakefield, *Mater. Sci. Eng., B*, 2010, **166**, 14–18.
- 16 D. C. Pan, S. C. Jiang, L. J. An and B. Z. Jiang, *Adv. Mater.*, 2004, **16**, 982–985.
- 17 D. L. Klayman and T. S. Griffin, *J. Am. Chem. Soc.*, 1973, **95**, 197–200.
- 18 M. Brust, M. Walker, D. Bethell, D. J. Schiffrin and R. Whyman, *J. Chem. Soc., Chem. Commun.*, 1994, 801–802.
- 19 D. C. Pan, Q. Wang, S. C. Jiang, X. L. Ji and L. J. An, *J. Phys. Chem. C*, 2007, **111**, 5661–5666.
- 20 D. C. Pan, Q. Wang, S. C. Jiang, X. L. Ji and L. J. An, *Adv. Mater.*, 2005, **17**, 176–179.
- 21 D. C. Pan, Q. Wang, J. B. Pang, S. C. Jiang, X. L. Ji and L. J. An, *Chem. Mater.*, 2006, **18**, 4253–4258.
- 22 D. C. Pan, Q. Wang and L. J. An, *J. Mater. Chem.*, 2009, **19**, 1063–1073.
- 23 C. B. Murray, D. J. Norris and M. G. Bawendi, *J. Am. Chem. Soc.*, 1993, **115**, 8706–8715.
- 24 I. Mekis, D. V. Talapin, A. Kornowski, M. Haase and H. Weller, *J. Phys. Chem. B*, 2003, **107**, 7454–7462.
- 25 D. V. Talapin, S. Haubold, A. L. Rogach, A. Kornowski, M. Haase and H. Weller, *J. Phys. Chem. B*, 2001, **105**, 2260–2263.
- 26 Q. Wang, D. Pan, S. Jiang, X. Ji, L. An and B. Jiang, *Chem.–Eur. J.*, 2005, **11**, 3843–3848.
- 27 Q. Wang, D. C. Pan, S. C. Jiang, X. L. Ji, L. J. An and B. Z. Jiang, *J. Cryst. Growth*, 2006, **286**, 83–90.
- 28 Q. A. Wang, D. C. Pan, S. C. Jiang, X. L. Ji, L. J. An and B. Z. Jiang, *J. Lumin.*, 2006, **118**, 91–98.
- 29 D. C. Pan, X. L. Ji, L. J. An and Y. F. Lu, *Chem. Mater.*, 2008, **20**, 3560–3566.
- 30 M. D. Garrett, A. D. Dukes, J. R. McBride, N. J. Smith, S. J. Pennycook and S. J. Rosenthal, *J. Phys. Chem. C*, 2008, **112**, 12736–12746.
- 31 M. A. Hines and P. Guyot-Sionnest, *J. Phys. Chem.*, 1996, **100**, 468–471.
- 32 W. Qin, R. A. Shah and P. Guyot-Sionnest, *ACS Nano*, 2012, **6**, 912–918.
- 33 N. P. Gurusinghe, N. N. Hewa-Kasakarage and M. Zamkov, *J. Phys. Chem. C*, 2008, **112**, 12795–12800.
- 34 G. Saygili, G. Unal, S. Ozcelik and C. Varlikli, *Mater. Sci. Eng., B*, 2012, **177**, 921–927.
- 35 M. M. Demir, D. Soyal, C. Unlu, M. Kus and S. Ozcelik, *J. Phys. Chem. C*, 2009, **113**, 11273–11278.









1 Authors Queries

Journal: TC

5 Paper: c3tc00077j

Title: Developing a facile method for highly luminescent colloidal CdS_xSe_{1-x} ternary nanoalloys

Editor's queries are marked like this... **1**, and for your convenience line numbers are inserted like this... 5

Query Reference	Query	Remarks
1	For your information: You can cite this article before you receive notification of the page numbers by using the following format: (authors), J. Mater. Chem. C, (year), DOI: 10.1039/c3tc00077j.	
2	Please carefully check the spelling of all author names. This is important for the correct indexing and future citation of your article. No late corrections can be made.	
3	Please check that the inserted GA image and text are suitable.	
4	The labels given in Fig. 2 for the compositions of the nanoalloys are unclear. For clarity to the reader please can you provide a figure with clearer labels (preferably at 600 dpi, TIF format).	
5	Please check that changes to the English in the section beginning "The composition was..." have not affected the meaning.	
6	The meaning of "The selenium-rich core..." is not clear - please clarify.	
7	Ref. 36 is cited within the text but does not appear to be included in the reference list. Do you wish to add this reference to the reference list or would you like the citations to be removed from the text?	